

Modelization of lifetime measurement in the presence of radiation trapping in solid-state materials

S. Guy*

Laboratoire de Physico-Chimie des Matériaux Luminescents, Université Lyon 1, UMR 5620 du CNRS, Domaine Scientifique de la Doua, 10, rue André-Marie Ampère, 69622 Villeurbanne Cedex, France

(Received 10 January 2006; published 4 April 2006)

Radiation trapping causes significant lengthening of the measured fluorescence lifetimes in solid samples, which leads to overestimating them. Self-absorption inside solid-state samples is considerably enhanced by successive total internal reflections at the sample/air interface. A simple method for quantitative estimation of radiation trapping in solid-state materials within the frame of the Holstein-Biberman equations is presented. This method is based on the assumption that the radiation propagation follows paths with many total internal reflections; it can be applied to many resonant two-level systems such as Er^{3+} -, Yb^{3+} -, or Ho^{3+} -doped materials. The equations are solved for a pulsed excitation localized in a finite volume inside the sample. In our modeling approach, we take into account the initial geometric population distribution and the imaging setup. We derive analytical expressions of the measured decays, which give the deformation of the measured curves compared with the ideal exponential decay. We investigate the effect of the fraction of self-trapped light on the decay modification. We then show that the ratio between the pumping volume, the collected volume, and the sample dimension changes the measured decay significantly.

DOI: [10.1103/PhysRevB.73.144101](https://doi.org/10.1103/PhysRevB.73.144101)

PACS number(s): 78.20.Bh

INTRODUCTION

Repeated incoherent processes of resonant absorption and emission of radiation in a medium influence substantially its spectral and dynamic features. The process of radiation trapping is well known to be responsible for an increase of the excited-state population lifetime beyond the natural lifetime of an individual emitter. Radiation trapping in gases has been intensely studied since its first description by the Holstein-Biberman (HB) equation^{1,2} (see the review by Molish and Oehry³).

In the case of a solid luminescent material, the reabsorption effect is well known to lengthen the measured lifetime.⁴⁻⁸ Moreover, it can change the shape of the emission spectra and thus influence quantum efficiency or light yield measurements.^{4,8,9} These results may be divided into two categories depending on the sample size compared with the absorption length of the radiation. For short absorption length, the propagation inside the sample between the excitation region and the detection region is long enough to allow many absorption-emission events. So this distance is the main parameter responsible for the lifetime lengthening and the deformation of the emission spectra.^{4,7,9} For lightly doped materials, lifetime lengthening can be observed even though there is no significant absorption for one pass through the sample. In many rare-earth materials, measured lifetime values are rather scattered. For example Zhang and Pun¹⁰ reported a $^4I_{13/2}$ measured lifetime in Er^{3+} -doped LiNbO_3 between 2.2 and 4.6 ms. In Yb^{3+} -doped yttrium aluminum garnet (Yb^{3+} :YAG) also, measured lifetimes were reported as 950,¹¹ 1080,¹² 1160,¹³ or 1300 μs .¹⁴ Here, self-absorption effects occur because an important fraction of the light produced within the sample is trapped in the material by total internal reflection (TIR). Shurcliff calculated precisely the amount of trapped light produced within rectangular paral-

lelepipeds, plane parallel sheets, and sphere.¹⁵ For rectangular parallelepipeds and spheres of refractive index 1.5 (standard glass) the trapping fraction is, respectively, 0.236 and 0.414. In a YAG crystal ($n \sim 1.8$), these numbers are as large as 0.494 and 0.575 for parallelepipeds and spheres. Ideally, this circulating light can undergo an infinity of TIRs and so will eventually be reabsorbed by the active centers. In real objects, however, imperfection and scattering effects destroy the "perfect" path allowing the light to escape from the sample.

Because a prerequisite for quantum efficiency and cross section determination is an unambiguous lifetime determination, quantifying and reducing radiation trapping is of prime importance. Some authors proposed an experimental setup to reduce radiation trapping effects in rare-earth-doped materials. The idea is to suppress the infinity of TIRs by surrounding the observed sample with an index-matched material, which allows the light to escape from the luminescent sample. Hehlen placed a small sample at the center of a large index-matched sphere^{11,16} in such a way that all the light rays coming from the sample hit the sphere periphery normally. Another setup, used for Yb :YAG (Ref. 5) and Er : LiNbO_3 ,^{10,17} consists in a thin plate of doped material sandwiched between two index-matching undoped pieces of the same material. In that case, not only the index-matched interface structure but also the excitation and emission collection arrangement has a dramatic impact on the measured lifetime: fluorescence was collected through an adjustable aperture imaging only the pumped zone and investigation of the excitation and emission collection scheme showed the dramatic effect of the aperture size.¹⁰ These methods give good results: a reduction of the measured lifetime of more than 30% is obtained in the case of the index-matched arrangements compared with non-index-matched measurements.

To our knowledge, only a few papers deal with the theoretical analysis of the radiation trapping effect in luminescent solid materials. This problem is very difficult because the resonant population at one point can be excited due to absorption of radiation emitted elsewhere. Since the absorption coefficient strongly depends on the radiation frequency, the theoretical description cannot be reduced to the diffusion equation and the transport problem becomes nonlocal.

Birks *et al.*¹⁸ and Caird *et al.*⁸ gave an expression of the measured lifetime and of the measured quantum efficiency by simply counting the number of photons effectively escaping from the emitting sample after an infinite succession of absorption and emission events inside the sample. Assuming that a fraction f of the emitted light is trapped inside the studied body after each absorption event, they found that the measured lifetime is given by

$$\tau^* = \frac{\tau}{1 - \eta f} \quad (1)$$

where τ and η are the intrinsic lifetime and quantum efficiency of the system. The main point of this model is that all the photons escaping from the system are collected by the measurement setup. Moreover, there is no need of any assumption about the excitation distribution.

Nelson and Sturge,¹⁹ in their work on Cr^{3+} , used the strongly self-absorbed R line to measure the emission arising from the vibronic transitions. Considering that the R line is monochromatic in comparison with the vibronic transition, they used the diffusion equation to describe the radiation transport. Then, assuming a uniform excitation distribution, they found the same analytical expression of the measured lifetime as Eq. (1). This approach was used later by Auzel *et al.*²⁰ in the limit of weak absorption; their result is the Taylor expansion of Eq. (1). Monte Carlo simulation on a spatially homogeneous excitation density presents a similar dependence for the measured lifetime.^{16,21}

The use of local diffusion equations limits the study to monochromatic ($\lambda_{em} = \lambda_{abs}$) radiation or weakly doped systems. The assumptions of homogeneous population distribution and collection of the whole light escaping from the sample are not adapted to practical laboratory conditions, for which excitation and collection setup are critical.^{5,10,17} Indeed, as the pump source generally excites only one part of the sample, two very different kinds of emission can be detected: the direct emission from excitations located in the pumped region and the indirect emission from excitations located outside the pumped region and excited by the first-generation emission. Thus, the excitation and collection scheme plays a dramatic role on lifetime measurements as demonstrated by the experimental work of Munoz *et al.*¹⁷ and Zhang,¹⁰ who showed that a doubling of the lifetime may be observed.

The purpose of this paper is to give a more precise description of radiation trapping in solid-state materials taking into account the experimental conditions corresponding to the excitation and collection setup. In our approach to the problem, we begin by using the HB equation and calculate the resonant radiation transport for an Er^{3+} -doped glass. This

system was chosen as a numeric example, but the results presented here can be used for other resonant transitions in solid materials. We show that the resonant radiation transport in highly symmetrical samples is governed by many TIRs, which makes the energy deposition uniform (Sec. I). Then, we solve the radiation transport in the particular case of transport governed by many TIRs. We take into account the fact that the laser beam pumps a localized region inside the sample. The rest of the sample is excited via the emission from the laser-pumped zone. The resolution of the integro-differential HB equation allows one to determine the evolution of the excited population in these two zones (Sec. II A). We use these solutions to describe the usual experimental situation of decay measurements with collecting optics (Sec. II B). We then show that the experimental setup, via the volume of excitation and collection, lengthens the decay curves, as much as the fraction of trapped light does. The special case of a quantum efficiency measurement with an integrating sphere is treated in Sec. II B 3.

I. THE RADIATIVE TRANSPORT EQUATION

A. The Holstein-Biberman equation

In the following, we recall the main result of the so-called Holstein-Biberman equation, which describes the evolution of the resonant excited-state density in the presence of resonant radiation.^{1,2} We use the following assumptions: emission is isotropic; ions are considered as two-level systems (i.e., ground state and resonant excited state); the excited-state population is much lower than the ground-state population; the processes of emission and absorption are independent; the flight times of photons are negligible compared with the natural lifetime of the excited state. In the case of radiation transport, the population density of resonant excited states is described by the equation

$$\frac{\partial n(\vec{r}, t)}{\partial t} = -\frac{1}{\tau}n(\vec{r}, t) + W_r \int n(\vec{r}', t)G(\vec{r}', \vec{r})d^3r'. \quad (2)$$

The first term of the right-hand side part is the natural decay of the considered population. It is related to the radiative and nonradiative deexcitation probabilities W_r and W_{nr} by $\tau^{-1} = W_r + W_{nr}$. The resonant transport is described by the integral term: the local population at \vec{r} is excited by the emission coming from everywhere else. $G(\vec{r}', \vec{r})$ is the probability that the radiation emitted at \vec{r}' is absorbed at \vec{r} at a distance $\rho = |\vec{r}' - \vec{r}|$:

$$G(\rho) = -\frac{1}{4\pi\rho^2} \frac{\partial T}{\partial \rho}. \quad (3)$$

For a nonmonochromatic emission, the averaged transmission $T(\rho)$ is given by the Beer-Lambert law averaged via the probability $P_e(\lambda)$ that a photon is emitted at wavelength λ :

$$T(\rho) = \int P_e(\lambda) e^{-N\sigma_a(\lambda)\rho} d\lambda \quad (4)$$

where σ_a is the absorption cross section and N the concentration. $P_e(\lambda) = I_e(\lambda) / \int I_e(\lambda) d\lambda$ is the normalized emission spectrum.

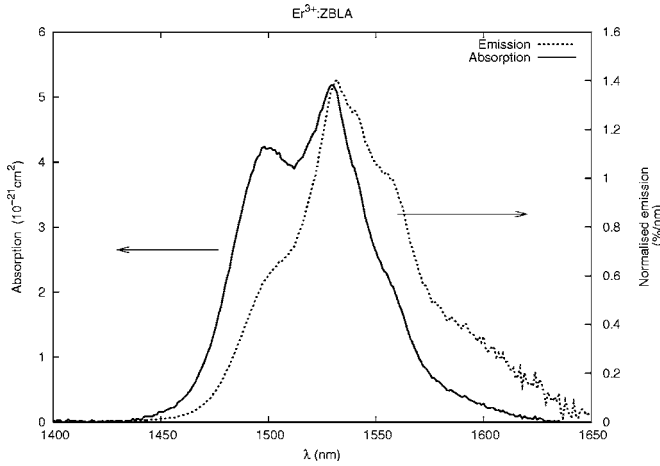


FIG. 1. Spectral overlap: Absorption and emission spectra of a 1 at. % Er^{3+} -doped ZBLA glass measured at room temperature. The emission spectrum is normalized $[\int I_e(\lambda)d\lambda = 1]$ so that the intensity value at λ is the probability per nanometer that a photon is emitted at λ .

B. Transmission function

The averaged transmission function $T(\rho)$, which describes the radiation transport for a distance ρ , is the key parameter of Eq. (2). In the case of the gas phase, emission and absorption profiles can be analytically described, which leads to an analytical expression for $T(\rho)$.^{1,3} But in solids, no general analytical expression for the spectra can be derived. Thus the transmission function must be numerically computed from experimental spectra.

To get an idea of the radiation transport properties, we have recorded the absorption and emission spectra of the resonant ${}^4I_{15/2} \leftrightarrow {}^4I_{13/2}$ transition of an Er^{3+} -doped ZBLA glass ($\text{ZrF}_4\text{-BaF}_2\text{-LaF}_3\text{-AlF}_3$) (Fig. 1). From these emission and absorption spectra, $T(\rho)$ was computed using Eq. (4) and is drawn in Fig. 2 for three different concentrations. The resonant radiation transmission $T(\rho)$ follows an exponential law for short propagation distances and as the distance increases it departs from the exponential law, showing that a significant part of the radiation can propagate along a great distance without being absorbed.

In the case of weak opacity, i.e., $N\sigma_a(\lambda)\rho \ll 1$, for any distance and wavelength, the average transmission tends to an exponential function (dashed curves on Fig. 2). The equivalent cross section $\langle\sigma_a\rangle_{eq}$ is found by performing the expansion of the exponential Eq. (4):

$$\langle\sigma_a\rangle_{eq} = \int \sigma_a(\lambda)P_e(\lambda)d\lambda. \quad (5)$$

At weak opacity, the radiation transport can be approximated to a monochromatic transport with the cross section $\langle\sigma_a\rangle_{eq}$ and, in this case, the HB equation can be simplified to a diffusion equation.²²

From a theoretical point of view, the shapes of the transmission functions prevent one from defining a mean free path. It means that the averaged transmission cannot be written as the transmission of a unique emission wavelength.

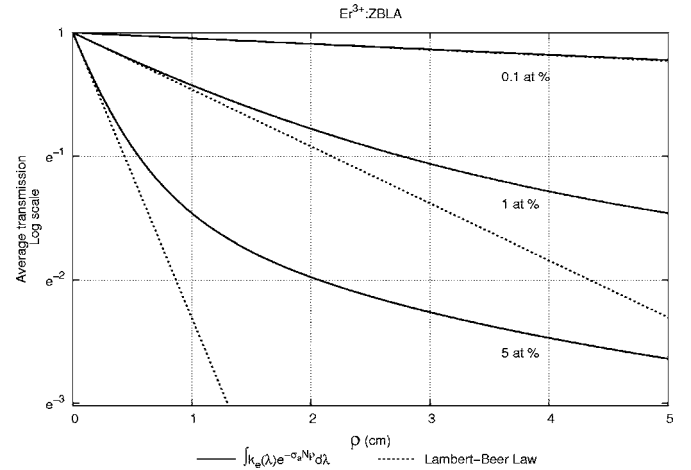


FIG. 2. Transmission function: Averaged transmission of the light emitted by the ${}^4I_{13/2}$ level for different erbium concentrations as a function of the propagation distance inside the doped sample. 1 at. % is 1.6×10^{20} at./ cm^3 in ZBLA. The dashed curves correspond to the approximation of weak opacity for which the transport is described as the transport of a unique emission wavelength (Beer-Lambert law).

And, by the way, the HB equation (2) cannot be reduced to a diffusion equation (Fick law). These properties are inherent to the definition of T [Eq. (4)] and do not depend on the exact nature of the emission and absorption spectra, providing that there is no correlation between absorption and emission processes.²² The curve shape does not depend on the overlap, only the length scale does. Thus, the results presented here can be applied to any resonant transition in rare-earth-doped materials.

C. TIR and self-absorption

In the case of luminescent solids, some part of the fluorescent light may be trapped within the sample because it is totally internally reflected at the interfaces. For a transparent highly symmetrical sample (parallelepiped, sphere), the TIR leads to infinite paths inside the sample.¹⁵ If these materials are doped with a resonant atomic level such as Er^{3+} or Yb^{3+} ions, the resonant radiation transport will satisfy the HB equation with the resonant radiation transmission function drawn on Fig. 2. Thus, for infinite samples, the resonant light travels a much longer distance than that which can be calculated from the maximum absorption cross section. Two physical processes lead to a dramatic increase of the light travel distance: first, at short distances, the averaging of the absorption through the whole emission and, second, at long distances, emission of photons in the weak-overlap wavelength range. A numerical example emphasizes this point. For 5 at. %, the absorption length defined as the length leading to $1/e$ transmission reduction is ~ 0.25 cm for light propagating at the maximum absorption-cross-section wavelength. The equivalent cross section $\langle\sigma_a\rangle_{eq}$ increases the absorption length to 0.4 cm and from the calculated curve in Fig. 2, there is still 7% of the light remaining after a 5 cm propagation. This last value would correspond to an absorp-

tion length of ~ 1.9 cm for an exponential propagation.

Then, for a standard experimental situation with sample size in the order of a few millimeters and concentration lower than some percent, the light effectively undergoes many TIRs before being absorbed. Furthermore, the energy redeposition inside the body is unpredictable and we may assume that there is no correlation between the emission point and the absorption point. Thus, the kernel function is uniform across the sample. With f being the fraction of trapped light and V_s the sample volume, the function $G(\rho)$ may be simplified as

$$G(\rho) = G = \frac{f}{V_s}. \quad (6)$$

For ideal bodies of high symmetry, the fraction of trapped light can be calculated from geometrical considerations¹⁵ and does not depend on absorption considerations. For practical situations, surface irregularities and imperfect volume homogeneity may deflect light rays from trapping paths to non-trapping paths. Thus the fraction of trapped light will be smaller than in the ideal case and will depend on the effective absorption cross section ($\langle\sigma_a\rangle_{eq}$ for weak absorption), the effective length, and the concentration, as already stated by Auzel *et al.*²⁰ Nevertheless, the assumption leading to Eq. (6) is still valid, providing that many TIRs occur before an absorption event occurs. This assumption is validated by the experimental studies on lifetime measurements in $\text{Yb}^{3+}:\text{YAG}$ and $\text{Er}^{3+}:\text{LiNbO}_3$ samples, which have demonstrated that the rare earth lifetime for different doping levels and boxlike geometry is governed by many TIRs.^{5,10,11,17}

II. EFFECT OF RADIATION TRANSPORT ON DECAYS IN SMALL AND LIGHTLY DOPED SAMPLES

A. Modeling of the physical processes

We model the experimental situation as follows. The sample volume V_s contains a resonant two-level system population (i.e., ground state and resonant excited state), the volume V_e inside the sample is excited at time $t=0$, and the detection system records the evolution of the excited population inside the collected volume V_c , which includes the initial excited part of the sample (see Fig. 3). In this section, we are interested in the evolution of the excited population density after the initial spatially localized excitation. We limit ourselves to the case where the radiation transport is governed by many TIRs. This is satisfied for low to standard doping levels in rare-earth-doped high-symmetry samples in the range of a few mm.^{5,11}

We have to solve the HB equation with the initial conditions for the excited-state population density

$$n(r, t=0) = \begin{cases} n_e^0 & \text{if } r \in V_e, \\ 0 & \text{if } r \notin V_e. \end{cases} \quad (7)$$

The directly excited population in volume V_e will decay and a part f of the emission excites the initially nonexcited volume via resonance radiation absorption. This volume also excites the initially excited one via resonance radiation absorption. Because the kernel function G is constant, the ini-

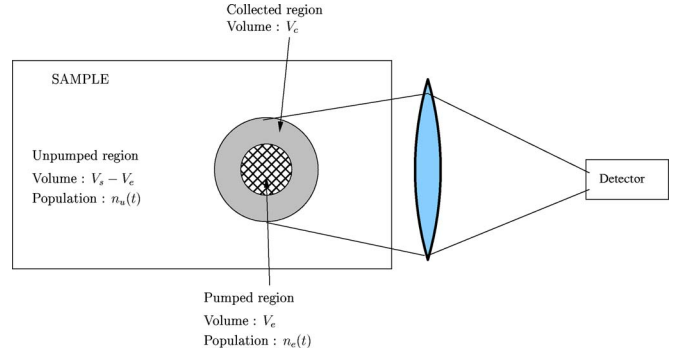


FIG. 3. (Color online) Geometric setup: The excitation source is focused in the hatched volume V_e inside the sample volume V_s . The collecting setup images the gray volume V_c centered on the pumped region onto the detector.

tial distribution splitting remains during the whole process, leading to the two coupled populations

$$n(r, t) = \begin{cases} n_e(t) & \text{if } r \in V_e, \\ n_u(t) & \text{if } r \notin V_e. \end{cases} \quad (8)$$

The equations governing these two populations coupled by radiation transfer can be written by inserting the constant value of G in Eq. (2) for the two regions. The integrals are simplified, showing that the two populations are governed by the following rate equations:

$$\frac{dn_e}{dt} = \left(-\frac{1}{\tau} + W_r G V_e \right) n_e + W_r G V_u n_u, \quad (9a)$$

$$\frac{dn_u}{dt} = \left(-\frac{1}{\tau} + W_r G V_u \right) n_u + W_r G V_e n_e. \quad (9b)$$

This is a linear system describing two populations coupled together via the probability $W_r G$. The solution of this system with the initial conditions (7) is

$$n_e(t) = e^{-t/\tau} n_e^0 + n_u(t), \quad (10a)$$

$$n_u(t) = \frac{V_e n_e^0}{V_s} (e^{-t/\tau^*} - e^{-t/\tau}), \quad (10b)$$

where $\eta = \tau W_r$ is the intrinsic quantum efficiency of the system and τ^* is defined by

$$\tau^* = \frac{\tau}{1 - \eta f}. \quad (11)$$

In the pumped region, the population density is the sum of two dynamic contributions corresponding to two excitation processes: the laser exciting process with the natural exponential decay of lifetime τ and the self-absorbed exciting process $n_u(t)$ with two exponential components (rise time τ and decay τ^*). Outside the pumped region, only the indirect excitation remains. Thus, the population densities corresponding to each of the two regions present very different dynamics as shown in Fig. 4. The indirect-excitation population density [Eq. (10b)] presents an initial rising before decaying. Its intensity is proportional to the number of laser-

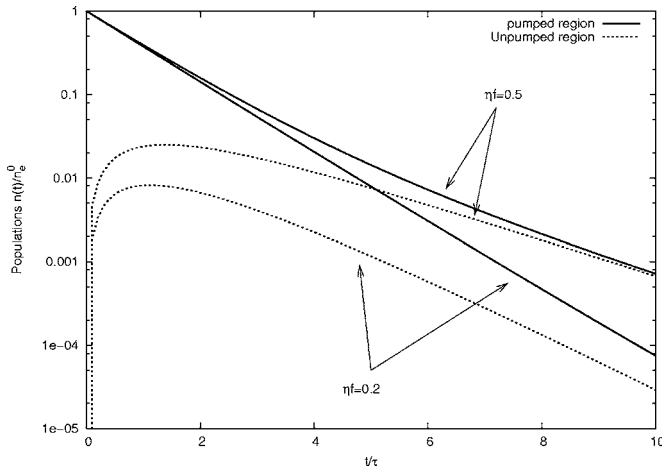


FIG. 4. Evolution of the excitation densities inside and outside the pumped region after a pulsed excitation localized in the pumped region. The initial population density inside the pumped region is n_e^0 . The unpumped region is populated via the radiation transport coming from the initially pumped region. We assume that the radiative energy redeposition governed by many TIR paths is constant. Curves are calculated for a ratio of the pumped volume over the sample volume equal to 10%.

excited photons $V_e n_e^0$ times the probability to be reabsorbed $G \sim 1/V_s$. The maximum is reached at time

$$t_{max} = -\tau \frac{\ln(1 - \eta f)}{\eta f}. \quad (12)$$

The population dynamics in the pumped region [Eq. (10a)] is nearly exponential at short times and deviates from the exponential law at longer times. The deviation is more and more pronounced as the ratio between the self-absorption and the laser excitation processes increases. As shown in system (10), this ratio is proportional to V_e/V_s .

B. Measured decay curves

In a typical experiment, the laser excites a sample volume V_e . Collecting optics image a zone of the sample, which includes the laser-excited zone, in the detectors as is presented schematically in Fig. 3. If the collecting zone includes only the first excited volume or only its complementary part, the decay is given directly by expression (10a) or (10b), respectively. But, in standard experiments, the optics collect a volume V_c including the initial excitation volume and a surrounding zone ($V_e < V_c < V_s$). Thus, the observed decay is a mixture of the dynamics of the directly and indirectly excited populations given by Eq. (10). By adding the contribution of the two populations in the two zones, the number of photons escaping from the sample at each time is

$$\Phi(t) = W_r(1 - f)[V_e n_e(t) + (V_c - V_e) n_u(t)]. \quad (13)$$

By using the expression (10), we find

$$\Phi(t) = [(1 - \alpha)e^{-t/\tau} + \alpha e^{-t/\tau^*}] \Phi(0) \quad (14)$$

where $\alpha = V_c/V_s$ is the collecting ratio and $\Phi(0) = W_r(1 - f)n_e^0 V_e$.

In our modelization of the experimental problem, the collected volume contains the pumped volume ($V_e < V_c < V_s$); thus the coefficient α varies between V_e/V_s and 1 and is controlled by the collecting setup. If the collecting setup images a region inside the pumped zone, the decay is directly given by the population $n_e(t)$ [Eq. (10a)]. Formally it is the same as 14 with $\alpha = V_e/V_s$. In this case, the coefficient α is controlled by the pumped setup. Finally to take into account the two situations we define α as

$$\alpha = \begin{cases} \frac{V_c}{V_s} & \text{if } V_e \subseteq V_c \\ \frac{V_e}{V_s} & \text{if } V_c \subseteq V_e \end{cases} = \frac{\max(V_c, V_e)}{V_s}. \quad (15)$$

The measured decay is the sum of two exponential decays: the intrinsic decay with the lifetime τ weighted by $1 - \alpha$ and a slower decay with the lifetime τ^* weighted by α .

In order to quantify the trapping effect on decay, we have calculated the integral lifetime $\int \Phi(t) dt / \Phi(0)$ from the previous Eq. (14):

$$\tau_{int} = \left(1 + \frac{\alpha \eta f}{1 - \eta f}\right) \tau. \quad (16)$$

The expression of the measured decay [Eq. (14)] as well as τ_{int} shows that two parameters control the observed decay: α which takes into account the experimental setup and ηf which counts the fraction of photons reemitted after a self-absorption step, i.e., the fraction of recycled light. We shall discuss the impact of these two terms in the next two sections. Beforehand, we can see that these two parameters α and ηf have a similar impact on the decay when they are small. For this purpose, we have calculated the $1/e$ lifetime when $\alpha \ll 1$ and $\eta f \ll 1$ by developing the exponential. In this limiting case, τ_{int} and $\tau_{1/e}$ are identical with the value

$$\tau_{1/e} = (1 + \alpha \eta f) \tau. \quad (17)$$

For small values of α and ηf , radiation trapping induces a lengthening of the lifetime proportional to the product $\alpha \eta f$.

1. Impact of the recycled light ηf

Mathematically, when ηf increases from 0 to 1, the time constant τ^* increases from the intrinsic lifetime τ up to infinity. So, the slow component of the measured decay will become slower and slower. The effect is more pronounced when the collecting factor is larger: more light comes from the unpumped region. Figure 5 illustrates the impact of the trapped light on the shape of the decays for two values of the collecting ratio: the larger ηf , the slower the measured decay. The variation of the integral lifetime versus ηf is drawn in Fig. 6. When ηf tends to zero, the measured lifetime tends to the intrinsic lifetime. When ηf tends to 1, the measured lifetime tends to infinity because the light is really trapped inside the sample and takes an infinite time to escape from the sample.

The dependence on ηf instead of f alone shows that the fraction of quanta slowing down the decay is not the fraction trapped inside the sample (fraction f), but the fraction circu-

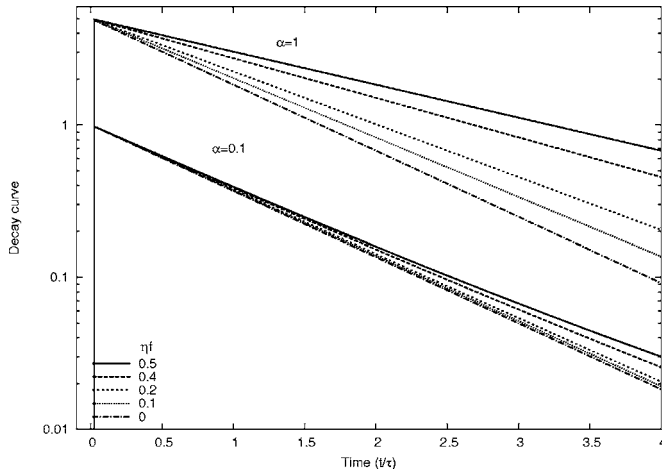


FIG. 5. Effect of the recycled light: Decay curves calculated from Eq. (14) as a function of ηf going from 0.5 to 0 for two values of the collecting ratio. ηf is the light fraction recycled inside the sample at each absorption or emission event. For $\alpha=0.1$, 10% of the sample is excited and imaged into the detector. $\alpha=1$ corresponds to the extreme case where the sample is either excited or imaged entirely.

lating indefinitely inside the system (trapped *and* reemitted). By the way, the dynamics of heavily doped systems with low quantum efficiency will not be affected too much by radiation trapping, although a large part of the light could be self-absorbed.

From a practical point of view, the trapping factor f is very difficult to quantify precisely because it depends on the exact absorption and emission overlap as well as on the sample geometry. Nevertheless, an estimation can be found for high-symmetry systems by considering the fraction of TIR at the interfaces.¹⁵ Another method proposed by Yin *et al.*²³ for Yb^{3+} -doped glasses is based on measured absorption spectra and emission spectra calculated using the reciprocity

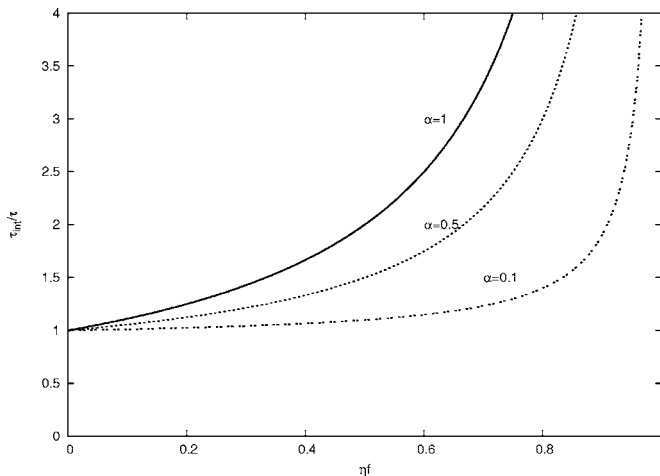


FIG. 6. Calculated integral lifetime τ_{int} as a function of the fraction of recycled light ηf . Three experimental setups are used: $\alpha=0.1$ (10% of the sample excited and imaged into the detector), $\alpha=0.5$ (50% of the sample excited and imaged into the detector), and $\alpha=1$ (the sample is excited or observed entirely).

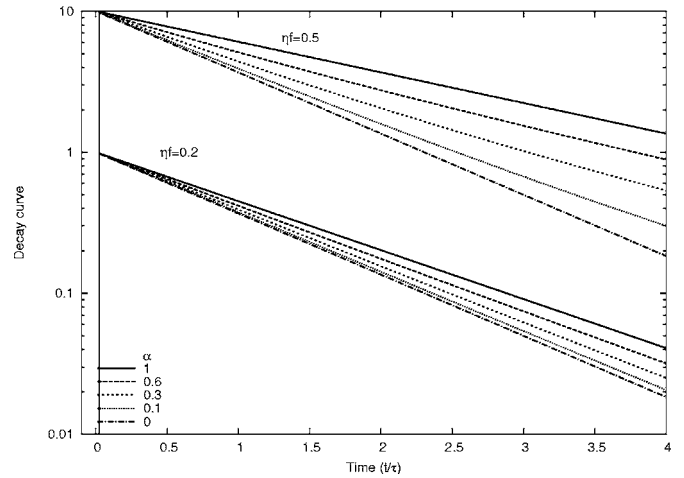


FIG. 7. Effect of the collecting setup: Calculated decay curves from Eq. (14) as a function of the collecting ratio $\alpha=\max(V_c, V_e)/V_s$ going from 1 to 0 for two values of recycling light ηf . The case $\alpha=0$ corresponds to the intrinsic decay with lifetime τ .

method. Because radiation trapping is eliminated in the calculated emission spectra it is possible to evaluate this effect by comparing the calculated and measured emission spectra.

2. Impact of the experimental setup

The experimental setup is taken into account via the α parameter, defined in Eq. (15), which measures the relative size between the maximum of the pumped or collected volume and the sample volume. As seen in expression (14), the impact of the ratio α is to change in the decay the relative weight between the slow component of lifetime τ^* and the intrinsic component of lifetime τ in favor of the slower one. When α goes from 0 to 1, the measured (extrinsic) decay shape varies continuously between that of the intrinsic decay with lifetime τ and that of the slower exponential decay with lifetime τ^* , as illustrated in Fig. 7. The integral lifetime increases linearly versus the collecting ratio α , from $\tau_{int}=\tau$ to $\tau_{int}=\tau^*$ when α goes from 0 to 1.

In practical cases, as a reduction of the radiation trapping is wanted, it is necessary to diminish the α ratio. Equation (15) defining α shows that the pumped volume and the collected volume must fit together. The best result is obtained when both the collected volume and the pumped volume are small (and identical) in comparison with the sample volume. This corresponds to a confocal setup. In this case, most of the detected photons come from the first-generation emission because the second-generation emission has little chance to be reabsorbed in the small initially excited or detected region compared with the rest of the sample.

On the other hand, when the collected or the pumped volume is the sample volume, the measured decay is the sum of all the first- and second-generation emissions and consists in a single exponential with the lifetime τ^* . This is the situation where the radiation trapping effect is maximum. We find again here the lifetime lengthening previously calculated

in the limiting cases of uniform excitation¹⁹ ($V_e=V_s$) and complete collection^{8,18} ($V_c=V_s$).

The experimental study¹⁰ of the excitation collection scheme in Er³⁺-doped LiNbO₃ can be directly compared with our theoretical work because it uses the same experimental setup as the one given in Fig. 3. The fluorescence is collected through an adjustable aperture which allows us to control what we call the α parameter. It was found that, for small aperture diameters ($\alpha < 1/200$), the measured decays do not depend on the concentration in the range 0.5% up to 2%, as described by Eq. (16). As the aperture diameter increases, the concentration dependence appears and the measured lifetime is nearly doubled for large aperture and concentration. The variation of the measured lifetime versus the aperture size seems to be linear for small apertures and quadratic, as expected from our work, for large apertures.

3. Quantum efficiency

For quantum efficiency measurements, luminescent samples are centered in an integrating-sphere and the number of absorbed photons of the exciting laser is compared to the number of emitted photons.⁸ In this kind of experiment, all the photons coming from the sample are detected wherever they are coming from. Within the frame of our model, it corresponds to the case $\alpha=1$, for which the collected volume equals the sample volume.

Intrinsic quantum efficiency is responsible for a diminution of the number of emitted photons compared with the number of excitations. When radiation trapping effects occur, each generation of reabsorbed photons leads to extra losses, leading to a decrease of the experimental quantum efficiency. The measured quantum efficiency η^* is the number of emitted photons escaping from the sample [i.e., $\int \Phi(t)dt$] divided by the number of initial excitations (i.e., $n_e^0 V_e$). Thus, it is directly given by $W_r(1-f)\tau_{int}$. By using Eq. (16) with $\alpha=1$ we get

$$\eta^* = \eta \frac{1-f}{1-\eta f}. \quad (18)$$

Figure 8 shows the dependence of the measured quantum efficiency on both the intrinsic quantum efficiency and the trapping factor for the integrating-sphere setup ($\alpha=1$). We can notice that radiation trapping has no effect when the quantum efficiency is 1; in this case the impact of trapping is only to delay the emission.

We find the same result [Eqs. (18) and (11)] as in the model developed by Birks^{18,24} and later used by Caird *et al.*⁸ This model described radiation trapping as a succession of reabsorption processes with an overall efficiency f leading to a measured quantum efficiency η_m given by

$$\eta_m = \eta(1-f) + (\eta f)\eta(1-f) + (\eta f)^2\eta(1-f) + \dots \quad (19)$$

where the first term on the right-hand side accounts for the first-order emitted photons escaping from the sample, the second term accounts for the first-order reabsorbed photons escaping the sample, the third term accounts for the second-order reabsorbed photons escaping the sample, and so on. In

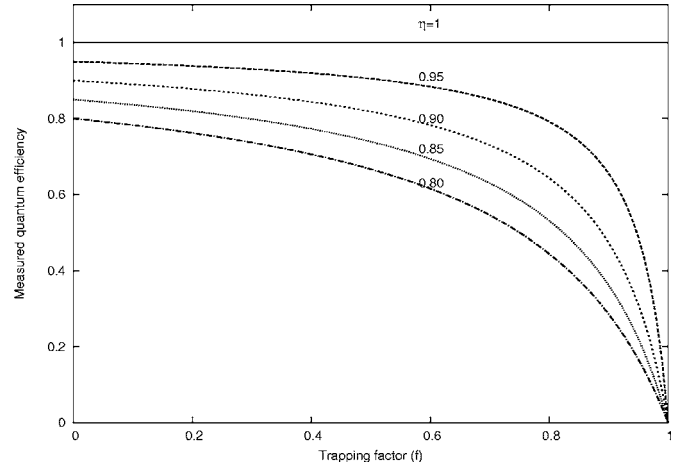


FIG. 8. Calculated observed quantum efficiency versus the overall trapping factor for different values of the intrinsic quantum efficiency.

this approach, the authors count the overall effect of the radiation trapping in the whole of the sample. By that way, it is equivalent to our description when we perform the integration of the population distribution over the whole of the sample.

CONCLUSION

We have derived a general expression of the measured decay curves in the case of solid-state self-absorbing materials. The main assumption is that the resonant radiation transport is mainly due to many unpredictable TIRs at the interfaces. We model the experimental conditions by dividing the studied sample into two regions: the initially excited region and its complementary part. The solution of the transport equation shows that the evolution of the population distribution inside the sample is the combination of two components: the natural decay localized inside the pumped region and the indirect decay evenly distributed inside the sample.

Experimental decays are the result of light collected from different regions inside the sample. We have shown that the impact of the radiation trapping depends on three parameters: the quantum efficiency η , the fraction of trapped light f , and an experimental factor called α . The product of the first two parameters counts the number of photons which are re launched in the system after a self-emission or absorption event in the studied sample. The experimental parameter α takes into account the ratio of the direct emission versus the indirect emission recorded by the optical setup. In order to reduce the trapping effect on the observed decay curves, the excitation and collection volume must be identical and as small as possible.

ACKNOWLEDGMENTS

The author wishes to acknowledge Y. Guyot and C. Garapon for carefully reading the manuscript and having helpful discussions.

*Electronic address: guy@pcml.univ-lyon1.fr

- ¹T. Holstein, Phys. Rev. **72**, 1212 (1947).
- ²L. M. Biberman, Zh. Eksp. Teor. Fiz. **17**, 416 (1947).
- ³A. F. Molisch and B. P. Oehry, *Radiation Trapping in Atomic Vapours* (Oxford University Press, Oxford, 1998).
- ⁴A. Bensalah, Y. Guyot, A. Brenier, H. Sato, T. Fukuda, and G. Boulon, J. Alloys Compd. **380**, 15 (2004).
- ⁵D. S. Sumida and T. Y. Fan, Opt. Lett. **19**, 1343 (1994).
- ⁶Yujin Chen, Yidong Huang, and Zundu Luo, Chem. Phys. Lett. **382**, 481 (2003).
- ⁷L. Laversenne, Y. Guyot, C. Goutaudier, M. T. Cohen-Addad, and G. Boulon, Opt. Mater. **16**, 475 (2001).
- ⁸J. A. Caird, A. J. Ramponi, and P. R. Staver, J. Opt. Soc. Am. B **8**, 1391 (1991).
- ⁹C. Dujardin *et al.*, J. Phys.: Condens. Matter **10**, 3061 (1998).
- ¹⁰D. L. Zhang and E. Y. B. Pun, J. Appl. Phys. **94**, 1339 (2003).
- ¹¹M. P. Hehlen, in *OSA Topics on Advanced Solid State Lasers*, edited by S. A. Payne and C. Pollock (OSA, Washington, DC, 1996), Vol. 1, p. 530.
- ¹²L. D. DeLoach, S. A. Payne, L. L. Chase, L. K. Smith, W. L. Kway, and W. F. Krupke, IEEE J. Quantum Electron. **29**, 1179 (1993).
- ¹³P. Lacovara, H. K. Choi, C. A. Wang, R. L. Aggarwal, and T. Y. Fan, Opt. Lett. **16**, 1089 (1991).
- ¹⁴G. A. Bogomolova, D. N. Vylegzhanin, and A. A. Kaminskii, Sov. Phys. JETP **42**, 440 (1976).
- ¹⁵W. A. Shurcliff and R. C. Jones, J. Opt. Soc. Am. **31**, 912 (1949).
- ¹⁶M. Hehlen, J. Opt. Soc. Am. B **14**, 1312 (1997).
- ¹⁷J. A. Munoz, B. Herreros, G. Lifante, and F. Cusso, Phys. Status Solidi A **168**, 525 (1998).
- ¹⁸J. B. Birks, Phys. Rev. **94**, 1567 (1954).
- ¹⁹D. F. Nelson and M. D. Sturge, Phys. Rev. **137**, 1117 (1965).
- ²⁰F. Auzel, F. Bonfigli, G. Baldacchini, and G. Baldacchini, J. Lumin. **94–95**, 293 (2001).
- ²¹In this paper, curves describing the ratio τ^*/τ versus ηf have hyperbolic shape, which is expected from Eq. (1).
- ²²C. van Trigt, Phys. Rev. **181**, 97 (1969).
- ²³H. Yin, P. Deng, J. Zhang, and F. Gan, Mater. Lett. **30**, 29 (1997).
- ²⁴J. B. Birks, Proc. Phys. Soc. London **79**, 494 (1962).